Lipids (2018) **53:** 413–427
DOI 10.1002/lipd.12039

ORIGINAL ARTICLE

Lipidomic Study of Precursors of Endocannabinoids in Freshwater Bryozoan *Pectinatella magnifica*

Tomáš Řezanka[1] · Milada Vítová[2] · Jaromír Lukavský[3] · Karel Sigler[1]

Received: 20 September 2017 / Revised: 13 March 2018 / Accepted: 14 March 2018

Abstract Freshwater bryozoan *Pectinatella magnifica* was collected from a sand pit (South Bohemia). The total lipids after extraction from lyophilized bryozoans were analyzed using high-performance liquid chromatography/high-resolution negative tandem electrospray mass spectrometry. A total of 19 lipid classes were identified, including *N*-acyl-substituted phospholipids, that is, *N*-acylphosphatidylethanolamine and *N*-acylphosphatidylserine in their plasmenyl forms. Based on gas chromatography/mass spectrometry of 3-pyridylcarbonyl (picolinyl) esters, a very unusual fatty acid was identified, namely 24:7n-3 (all-*cis*-3,6,9,12,15,18,21-tetracosaheptaenoic acid). The presence of polyunsaturated fatty acids in individual classes is very specific: arachidonic and eicosapentaenoic acids being predominantly bound as amides in *N*-acyl phospholipids, that is, diacyl-*N*-acylphosphatidylethanolamines (NAPtdEtn), plasmenyl-*N*-acylphosphatidyl ethanolamines (PlsNAPtdEtn), diacyl-*N*-acylphosphatidylserines (NAPtdSer), and plasmenyl-*N*-acylphosphatidylserines (PlsNAPtdSer). While 24:6n-3 was identified in the *sn*-2 position of several phospholipids, 24:7n-3 was identified in only two plasmalogens, that is, PlsNAPtdEtn and PlsNAPtdSer. Thanks to the tandem mass spectrometry, we managed to identify the position of all acyl groups in both diacyl- and also in alkenyl-acyl-(plasmenyl) molecular species of *N*-acylphospholipids. The identification of the molecular species of *N*-acyl-substituted phosphatidylethanolamine and phosphatidylserine, including their plasmalogen forms, in the freshwater bryozoan *P. magnifica* has enabled the identification of endogenous cannabinoid precursors.

Keywords Endocannabinoids · Freshwater bryozoan · Lipidomics · Liquid chromatography/tandem high-resolution electrospray mass spectrometry *N*-acylphosphatidylethanolamines · *Pectinatella magnifica*

Lipids (2018) **53:** 413–427.

Abbreviations

CID	collision-induced dissociation
DAG	diacylglycerol(s)
DMA	dimethylacetal(s)
ECL	equivalent chain length
ESI	electrospray ionization
ESI–MS	electrospray ionization mass spectrometry
FA	fatty acid
FAME	fatty acid methyl esters
FT	Fourier transform
GC/MS	gas chromatography–mass spectrometry
HESI	heated electrospray interface
HILIC	hydrophilic interaction chromatography
HPLC	high-performance liquid chromatography
HPLC–MS^2/ESI^-	HPLC–tandem mass spectrometry negative electrospray ionization
HR	high resolution

Electronic supplementary material The online version of this article (doi:10.1002/lipd.12039) contains supplementary material, which is available to authorized users.

✉ Tomáš Řezanka
rezanka@biomed.cas.cz

[1] Laboratory of Fungal Genetics and Metabolism, The Czech Academy of Sciences, Institute of Microbiology, Vídeňská 1083, 142 20, Prague, Czech Republic

[2] Laboratory of Cell Cycles of Algae, Centre Algatech, The Czech Academy of Sciences, Institute of Microbiology, Opatovický mlýn, 379 81, Třeboň, Czech Republic

[3] Department of Plant Ecology, Biorefinery Centre of Competence, The Czech Academy of Sciences, Institute of Botany, Dukelská 135, 379 82, Třeboň, Czech Republic

IR	infrared
LC/MS	liquid chromatography–mass spectrometry
MS	mass spectrometry
NAPtdEtn	diacyl-*N*-acylphosphatidylethanolamines
NAPtdSer	diacyl-*N*-acylphosphatidylserines
NLS	neutral-loss scanning
PlsNAPtdEtn	plasmenyl-*N*-acylphosphatidyl ethanolamines
PlsNAPtdSer	plasmenyl-*N*-acylphosphatidylserines
PtdCho	phosphatidylcholine
PtdEtn	phosphatidylethanolamine
PtdIns	phosphatidylinositol
PtdSer	phosphatidylserines
PUFA	polyunsaturated fatty acid(s)
SIM	selected-ion monitoring
TAG	triacylglycerol(s)
VLCPUFA	very-long-chain polyunsaturated fatty acid

Introduction

Freshwater bryozoans are far less frequent than their marine counterparts (Massard & Geimer, 2007), which include more than 8000 existing species; by contrast, less than 100 species live in freshwater and *Pectinatella magnifica* is one of them.

P. magnifica (Leidy, 1851) is a freshwater bryozoan with an invasive character. It originates from the eastern part of the Mississippi River (from Ontario to Florida) but has recently spread all over the world. It forms colonies up to several feet in diameter created by a gelatinous matrix with hundreds of individual zooids. Under optimal conditions, the growth rate of the colonies is extreme. It has a significant impact on both the biology and ecology of water reservoirs (Balounová, Rajchard, Švehla, & Šmahel, 2011). In the South Bohemian ponds, the wet mass of the individual colonies reached over 1 kg while the weight of all the bryozoa fished from the pond was more than 100 kg of wet mass.

The content of lipids and fatty acids (FA) in individual bryozoans has been very rarely examined. Unlike the sponges, on which hundreds of articles have been published, there are only a few publications devoted to bryozoans. One of the first papers (Vyssotski, MacKenzie, & Scott, 2009) describing FA of the bryozoan of the genus *Flustra* sp. identified the major polyunsaturated fatty acids (PUFA), that is, 22:6n-3 and 20:5n-3. Other PUFA, for example, 22:5n-3, 20:4n-3, 20:4n-6, 18:4n-3, 16:4, and 16:3, were also present. The very-long-chain polyunsaturated fatty acid (VLCPUFA), nisinic acid (24:6n-3), was found in phosphatidylethanolamine (PtdEtn) at about 3% of the total FA. Based on gas chromatography (GC), the presence of other C24 PUFA was assumed.

A similar FA content was found in other marine bryozoans *Berenicea meandrina* and *Dendrobeania flustroides*, 24:4n-3 being present in minor proportion. Furthermore, a series of aldehydes identified as dimethylacetals (DMA), both saturated and monounsaturated from C16 to C19, have been described (Demidkova, 2010).

The freshwater bryozoan *Plumatella emarginata* has been analyzed for the FA content, which was similar to the FA content of marine bryozoans; the content of 20:4n-6 reached 2.7% of total FA (Makhutova et al., 2016). Heptadecanal has been identified as a major aldehyde in eight marine bryozoans (Berdyshev, Getmanova, Svetashev, & Kubanin, 1992), which demonstrates the presence of plasmalogen lipids as part of total lipids.

Plasmenyl-phospholipids that belong to plasmalogens are ether phospholipids characterized by the presence of the vinyl ether linkage at the *sn*-1 position and the ester linkage at the *sn*-2 position. In mammals, *sn*-1 hydrocarbon chains are derived from fatty alcohols 16:0, 18:0, or 18:1, while *sn*-2 is mostly esterified by PUFA (Goldfine, 2010). The most common head group in mammalian plasmalogens is ethanolamine, which forms plasmenylethanolamine (Nagan & Zoeller, 2001). Compounds of this type serve as precursors in the biosynthesis of endocannabinoids, compounds that affect endogenous cannabinoid receptors located in the brain of mammals and in the central and peripheral nervous system consisting of neuromodulatory lipids and their receptors that affect physiological processes including appetite, pain, mood, memory, and so on. One of the most well-known endocannabinoids is anandamide, which is chemically *N*-arachidonoylethanolamine. Related substances that were isolated have a structure of ethanolamides of unsaturated FA, for example, 8,11,14–20:3 or 7,10,13,16–22:4 (Braverman & Moser, 2012).

Enzymatic hydrolysis of endocannabinoids, as well as cannabinoid receptors and endocannabinoids have been described in various invertebrate species, for example, sea urchins, annelids, or cnidarians (Salzet & Stefano, 2002). These signal molecules appear to play multiple roles. In invertebrates, they have been shown to function in diminishing the sensory input, control of reproduction, feeding behavior, neurotransmission, and anti-inflammatory effects. Their identification in invertebrates has been primarily intended for genetic analysis of the presence or absence of functional orthologs in the genomes (McPartland, Matias, Di Marzo, & Glass, 2006). The studies identifying individual endocannabinoids or their biosynthetic precursors in invertebrates are rather scarce. As an example, Lehtonen, Reisner, Auriola, Wong, and Callaway (2008) described their presence in nematodes or *N*-acylethanolamines in *Caenorhabditis elegans* (Lucanic et al., 2011).

The use of lipidomic techniques for identifying biosynthetic endocannabinoid precursors has only been performed

in mammals (see, e.g. Astarita, Ahmed, & Piomelli, 2008; Guan, 2009; Guan, Li, Smith, Shaw, & Raetz, 2007; Hansen, Hansen, Bjørnsdottir, & Hansen, 1999). Among the endocannabinoid precursors are *N*-acyl-substituted PtdEtn and/or phosphatidylserine (PtdSer), less common phospholipids, although they are found in many different organisms, from yeast to mammalian brain (Guan et al., 2007). Identification of *N*-acyl phospholipids is now almost exclusively carried out using liquid chromatography–mass spectrometry (LC/MS). High-resolution electrospray ionization tandem mass spectrometry (HR-ESI–MS^2) is preferably used in both the positive and negative modes. This method can identify hundreds of molecular species, including the determination of acyl groups at *sn*-1, *sn*-2, and *N*-acyl positions. This paper presents the analysis of *N*-acyl derivatives of *P. magnifica* phospholipids using hydrophilic interaction chromatography (HILIC-LC/HR-ESI–MS^2). This technique enabled us to identify the position of all acyl groups in both diacyl-*N*-acylphosphatidylethanolamine (NAPtdEtn) and also in alkenyl-acyl-*N*-acylphosphatidylethanolamine (PlsNAPtdEtn) (i.e. plasmalogen form of NAPtdEtn) and similar derivatives of PtdSer, that is, diacyl-*N*-acylphosphatidylserine (NAPtdSer) and alkenyl-acyl-*N*-acylphosphatidylserine (PlsNAPtdSer) (plasmenyl NAPtdSer). Identification of the molecular species of *N*-acyl-substituted PtdEtn and PtdSer, including their plasmalogen forms, in the freshwater bryozoan *P. magnifica* has enabled the identification of endogenous cannabinoid precursors and the comprehensive elucidation of their biosynthesis, metabolism, and function.

Materials and Methods

Chemicals and Standards

1-(1*Z*-octadecenyl)-2-oleoyl-*sn*-glycero-3-phosphocholine (C18(Plasm)-18:1-PtdCho) and 1-(1*Z*-octadecenyl)-2-oleoyl-*sn*-glycero-3-phosphoethanolamine (C18(Plasm)-18:1-PtdEtn) were purchased from Avanti Polar Lipids, Inc., Alabaster, AL, USA, and 9(Z),12(Z),15(Z),18(Z)-tetracosatetraenoic, 6(Z),9(Z),12(Z),15(Z),18(Z)-tetracosapentaenoic, 6(Z),9(Z),12(Z),15(Z),18(Z),21(Z)-tetracosahexaenoic acids, and 2(E),6(Z),9(Z),12(Z),15(Z),18(Z),21(Z)-tetracosaheptaenoic acid methyl ester from Larodan (Malmö, Sweden). 1,2-Dipalmitoyl-diacylglyceryltrimethylhomoserine, di-all-*cis*-4,7,10,13,16,19-docosahexaenoyl-PtdCho, and 1,2-dioleoyl PtdIns (ammonium salt) were purchased from Avanti Polar Lipids, Inc., Alabaster, AL, USA. Digalactosyl diacylglycerol (DGDG), monogalactosyl diacylglycerol (MGDG), and sulfoquinovosyldiacylglycerol (plant leaf lipids), cholesteryl linoleate, 1,2-di-all-*cis*-4,7,10,13,16,19-docosahexaenoin, 1,2-dioleoyl-phosphatidic acid, 1,2-dioleoyl-PtdCho, 1,2-dioleoyl-PtdEtn, 1,2-dioleoyl-phosphatidylglycerol (Na-salt), tri-all-*cis*-4,7,10,13,16,19-docosahexaenoin, and 1,2-dimyristoyl-phosphatidylserine (Na-salt) from Larodan (Malmö, Sweden). All other chemicals were purchased from Sigma–Aldrich (Prague, Czech Republic).

Collection of Bryozoa

Samples were collected from the Cep sand pit (near Suchdol n.Lužnicí). The biomass, a jelly body, was frozen and stored at −20 °C, then lyophilized and stored also at −20 °C.

Isolation of Lipids

The extraction procedure was based on the method of Bligh and Dyer (1959), except that 2-propanol was substituted for methanol, as 2-propanol does not serve as a substrate for phospholipases (Kates & Volcani, 1996). The alcohol–water mixture was cooled, one part chloroform was added and the lipids from the lyophilized cells of different cultivations of yeasts were extracted for 30 min. The insoluble material was separated by centrifugation and the supernatant was separated into two phases. The aqueous phase was aspirated off and the chloroform phase was washed three times with two parts 1 M KCl each. The resulting chloroform phase was evaporated to dryness under reduced pressure.

Total lipid extracts were applied to Sep-Pak Vac Silica cartridge 35 cm^3 (Waters [Waters Gesellschaft m.b.H., Prague, Czech Republic]; with 10 g of normal-phase silica), and triacylglycerol (TAG) were subsequently eluted from the cartridge with 40 mL of chloroform:methanol (9:1). Polar lipids were eluted from the cartridge by a mixture of 50 mL of methanol acidified with 0.1% of formic acid. The eluate of polar lipids was evaporated and the oil samples were further hydrolyzed.

Analysis of Fatty Acid Methyl Esters and DMA

FA and fatty aldehydes were released from total lipids, see above, by acid hydrolysis (2 M HCl, 100 °C, 2.5 h), extracted with hexane, and methylated with 10% (w/v) methanolic BF_3 (80 °C, 10 min). GC–MS of the fatty acid methyl ester (FAME) and DMA mixture was done on a Finnigan (Finnigan, San Jose, CA, USA) 1020 B in the electron ionization (EI) mode. Splitless injection was carried out at 100 °C, and a fused silica capillary column (Supelcowax 10; 60 m × 0.25 mm i.d., 0.25 mm film thickness [Merck, Czech Republic]; Supelco, Prague, Czech Republic) was used. The temperature program was as follows: 100 °C for 1 min, subsequently increasing at 20 °C/min to 180 °C, and

at 2 °C/min to 280 °C, which was maintained for 1 min. The carrier gas was helium at a linear velocity of 60 cm/s. All spectra were scanned within the range of *m/z* 50–500. The structures of FAME were confirmed by the comparison of retention times and fragmentation patterns with those of the standard FAME (Supelco, Prague, Czech Republic) (Rezanka, 1990, 1993).

3-Pyridylcarbonyl Esters of FA

A solution of potassium *tert*-butoxide in tetrahydrofuran (0.5 mL, 1.0 M) was added to nicotinyl alcohol (1 mL). After mixing, the appropriate FAME (~0.5 mg) in dry dichloromethane (1 mL) were added, and the mixture was held at 40 °C for 30 min in a closed vial. After cooling to room temperature, water and hexane were added, and the organic phase was collected, dried over anhydrous sodium sulfate, and evaporated.

A FA 3-pyridylcarbonyl ester mixture was analyzed on the instrument described above. Injection temperature (splitless injection) was 100 °C, and an Ultra-1 capillary column (Supelco, Prague, Czech Republic) was used. The temperature program was as follows: 100 °C for 1 min, subsequently increasing at 20 °C/min to 180 °C and at 2 °C/min to 280 °C, which was maintained for 1 min. The carrier gas was helium at a linear velocity of 60 cm/s. All spectra were scanned within the range *m/z* 50–500.

HILIC-LC/MS–ESI

The high-performance liquid chromatography (HPLC) equipment consisted of a 1090 Win system (Agilent, Prague, Czech Republic), a PV5 ternary pump, an automatic injector (HP 1090 series; Hewlett Packard, Prague, Czech Republic), Ascentis® Express OH5 (Merck, Czech Republic), and a HPLC HILIC column (2.7 μm particle size, $L \times$ i.d. 15 cm × 2.1 mm) (Supelco, Prague, Czech Republic) with an injection volume of 10 μL. HPLC was performed at a flow rate of 0.33 mL/min for the polar lipids from three cultivations, with a linear gradient from the mobile phase containing methanol:acetonitrile:aqueous 1 mM ammonium acetate (50:30:20, v/v/v) to methanol:acetonitrile:aqueous 1 mM ammonium acetate (10:70:20, v/v/v) for 60 min. Column temperature was 35 °C and the re-equilibration period between runs was 30 min. The whole HPLC flow was introduced into the ESI source without any splitting.

LTQ Orbitrap Velos (Thermo Fisher Scientific, Bremen, Germany), a high-resolution hybrid mass spectrometer equipped with a heated electrospray interface (HESI), was used. ESI–MS analysis was performed in the Fourier transform (FT) positive-ion mode. MS spectra were acquired with a target mass resolution of $R = 105{,}000$ at *m/z* 800. The ion spray voltage was set at 3.5 kV and the scan range of the instruments was set at *m/z* 200–1500. Nitrogen was used as a nebulizer gas—set at 18 arbitrary units (sheath gas) and seven arbitrary units (auxiliary gas). Helium was used as a collision gas for collision-induced dissociation (CID) experiments. The CID normalization energy of 35% was used for the fragmentation of parent ions. The MS/MS product ions were detected in the high-resolution FT mode. Further source conditions in the positive mode were vaporizer temperature, 250 °C; capillary temperature, 230 °C; capillary voltage, 50 V; and tube lens voltage, 170 V. The isolation window was set to 1 Da (±0.5 Da), fragments were detected in the Orbitrap FTMS (Thermo Fisher Scientific, Bremen, Germany) mode with a resolution of 60,000 and mass accuracy better than 2 ppm.

The calibration of the MS spectrometer was done with the use of Pierce LTQ Orbitrap positive-ion calibration solution (ESI positive) and Pierce LTQ Orbitrap negative-ion calibration solution (ESI negative). Both calibration standards were provided by Thermo Scientific (Thermo Fisher Scientific, Bremen, Germany). For mass spectral acquisition, the internal lock mass was used: *m/z* 413.2662 $[M + Na]^+$-diisooctyl phthalate in ESI^+ and *m/z* 255.2330 $[M - H]^-$ palmitic acid in ESI^-. The mass accuracy was better than 3 ppm. Both ions were presented in the used mobile phase (LC/MS Chromasolv methanol [Honeywell Prague Laboratory, Praha, Czech Republic] and Millipore water [Merck Millipore, Burlingtong, MA, US]).

The same apparatus was used for the negative-ion mode. MS spectra were acquired with a target mass resolution of $R = 30{,}000$ at *m/z* 400. The ion spray voltage was set at −2500 V and the scan range of the instruments was set at *m/z* 200–2000. Nitrogen was used as a nebulizer gas—set at 18 arbitrary units (sheath gas) and seven arbitrary units (aux gas). Helium was used as a collision gas for CID experiments. The CID normalization energy of 35% was used for the parent ion fragmentation. The tandem MS product ions were detected in the high-resolution FT mode. The HESI temperature was set to 250 °C.

Statistics

Three replicates ($n = 3$) of each analysis were used. The software Statistica for Windows (version 12.0, Dell [Austin, TX, USA]) was used for analyses. Data were presented as means ± *SD*.

Results

Fatty Acids

Table 1 shows the FA content of the freshwater invertebrate *P. magnifica*. FA, and in particular PUFA, were identified

Table 1 Fatty acid (FA) (mol% of total FA) composition from three parallel collections of *P. magnifica*

FA	*P. magnifica*	±*SD*
14:0	1.9	0.09
14:1[a]	0.4	0.06
16:0	15.3	0.10
16:1n-9	2.4	0.07
16:1n-7	4.1	0.10
16:2n-4	2.2	0.06
16:3n-4	1.2	0.04
16:4n-3	1.1	0.05
18:0	6.1	0.09
18:1n-9	8.2	0.13
18:1n-7	3.3	0.07
18:2n-6	2.3	0.08
18:3n-3	2.7	0.09
18:4n-3	0.9	0.04
20:1n-9	1.1	0.05
20:1n-7	0.7	0.03
20:2n-6	2.1	0.06
20:3n-6	0.4	0.02
20:4n-6	5.5	0.08
20:4n-3	1.6	0.07
20:5n-3	13.2	0.12
22:0	0.6	0.06
22:1n-9	0.2	0.03
22:4n-6	0.3	0.02
22:5n-6	1	0.08
22:5n-3	1.4	0.11
22:6n-3	11.9	0.14
24:7n-3	2.1	0.08
24:6n-3	2.6	0.07
24:5n-6	1.1	0.05
24:5n-3	0.7	0.04
24:4n-6	0.2	0.02
24:4n-3	1.2	0.07
Dimethylacetal (DMA)		
16:0	23.8	3.78
17:0	31.6	2.41
18:0	44.6	5.63

[a]Position of the double bond was not determined.

using GC/MS of FAME on a polar capillary column. The position of the double bonds was based on fragmentation since it is known that the mass spectrum of n-3 PUFA methyl esters has an abundant ion at *m/z* 108 (Fellenberg, Johnson, Poulos, & Sharp, 1987). The PUFA structure was confirmed using 3-pyridylcarbinol esters (formerly called picolinyl esters). The mass spectra of these derivatives feature abundant ions at *m/z* 92, 108, 151 (the McLafferty rearrangement), and 164 Da. The structure can be determined on the basis of ions in which the 14 Da interval decrements are changed to the gap interval of 26 or 40 Da.

An example is the 3-pyridylcarbinol ester of 24:6n-3 acid (Fig. 1), whose mass spectrum showed a gap of 26 Da between *m/z* 418.3 and 392.3, which locates the double bond in position 21 while the gap between *m/z* 378.2 and 352.2 locates the double bond in position 18. Other gaps at *m/z* 338.2–312.2, 298.2–272.2, 258.1–232.1, and 218.1–192.1 unambiguously confirm the structure 24:6n-3. Among the other things, our mass spectrum is very similar to the mass spectrum published by Christie (2017).

GC/MS analysis further identified methyl ester having a very low-abundance $[M]^+$ at 368.3 Da, which suggests that it could be a 24:7 acid. Commercially available 2,6,9,12,15,18,21-tetracosaheptaenoic (2,6,9,12,15,18,21–24:7) methyl ester has the same mass spectrum as the methyl ester predetermined as 24:7, but has a different equivalent chain length (ECL) value. The natural ester has ECL 26.21, whereas the commercial standard has 26.86. For complete confirmation of the new structure, both the natural sample and the commercially available standard were converted to 3-pyridylcarbinol esters.

Fig. 2 shows the mass spectrum of the peak with ECL 26.21, that is, the natural 3-pyridylcarbinol ester of 24:7n-3. Gaps of 26 and 40 Da values are apparent in the mass spectrum of this compound, see the similarity to the mass spectrum of the shorter homolog, that is, 3-pyridylcarbinol-3,6,9,12,15-octadecapentaenoate (18:5n-3) (Christie, 2017). FA having the first double bond in the Δ^3 position are readily isomerized to compounds having double bond positions of 2, 6, 9, …. The mass spectra of these 3-pyridylcarbinol esters are, however, completely different and contain an abundant ion at *m/z* 177.1, which is formed by cleavage at the center of the *bis*-methylene interrupted double bond system (see Fig. 3). Therefore, we can safely say that our 24:7 PUFA has the structure of 3,6,9,12,15,18,21-tetracosaheptaenoic (24:7n-3) acid.

Other PUFA (see Table 1) were similarly identified. All double bonds have a *cis* (more recently *Z*) geometric configuration, as determined using the infrared (IR) spectra (Christie, 2003), as the IR spectrum completely lacks absorption of the CH bond in the range of 960–980/cm, that is, absorption of the double bond with a geometric *trans* configuration (more correctly *E*).

Separation and Identification of Lipid Classes, Including Molecular Species

Separation of commercially obtained lipid standards and total lipids of the bryozoan ("Materials and Methods") was performed by gradient elution on an HPLC column with the stationary phase containing OH groups. The lipid classes were mostly separated from the baseline both in the standard and in real samples, and the analysis lasted no

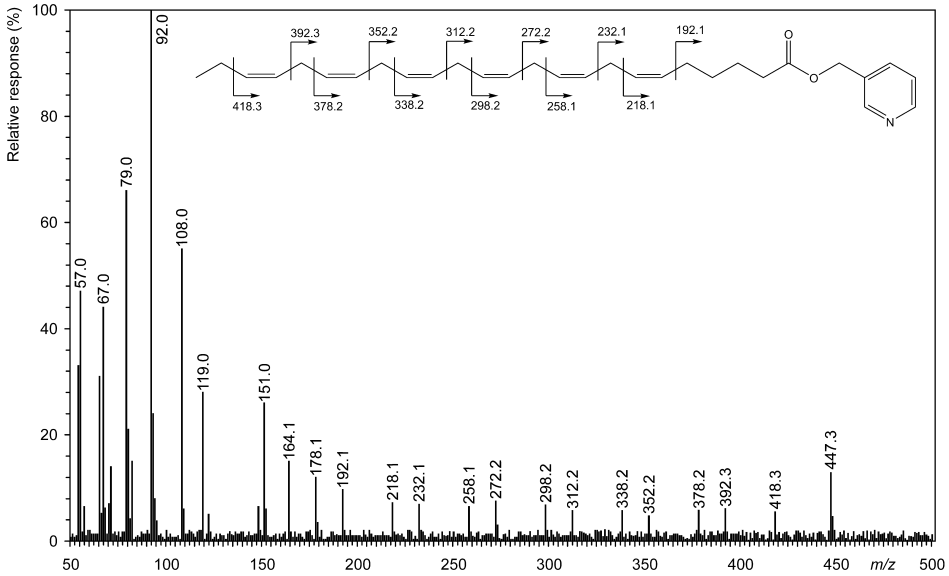

Fig. 1 The mass spectrum of 3-pyridyl carbonyl ester of 24:6n-3 acid

longer than 1 h (see Fig. 4). Identification was performed using negative ESI (ESI^-) and individual lipid classes were identified based on selected-ion monitoring (SIM) and neutral-loss scanning (NLS) using characteristic fragments generated in negative ESI. Virtually all classes of lipids have been separated, including plasmenyl-acyl and diacyl lipids. As can be seen from Fig. 4, the diol stationary phase provides partial intraclass separation leading to the division of individual molecular species. This separation is particularly noticeable for those molecular species that differ significantly in either the chain length or the number of double bonds. However, unlike interclass separation, the separation of molecular species in one lipid class was insufficient. A total of 25 lipid classes were separated, of which 19 were completely characterized. Unfortunately, we were not able to characterize the unknown lipids labeled C and F–J. Possible formation of artifacts resulting from the reaction of the free NH_2 group (ethanol amine and serine) can be completely avoided since *N*-acyls are essentially composed of only two PUFA, that is, 20:4 and 20:5 FA. If amides were formed during sample processing, a similar FA spectrum, to that in total acids, should be present in the *N*-acyls (see Table 1).

Fig. 4 shows the separation of lipid subclasses from *P. magnifica* by means of total ion current and also two methods of detection—NLS and SIM. In the case of neutral lipids and phospholipids comprising PUFA, we also made further identification by tandem MS. Based on the presence

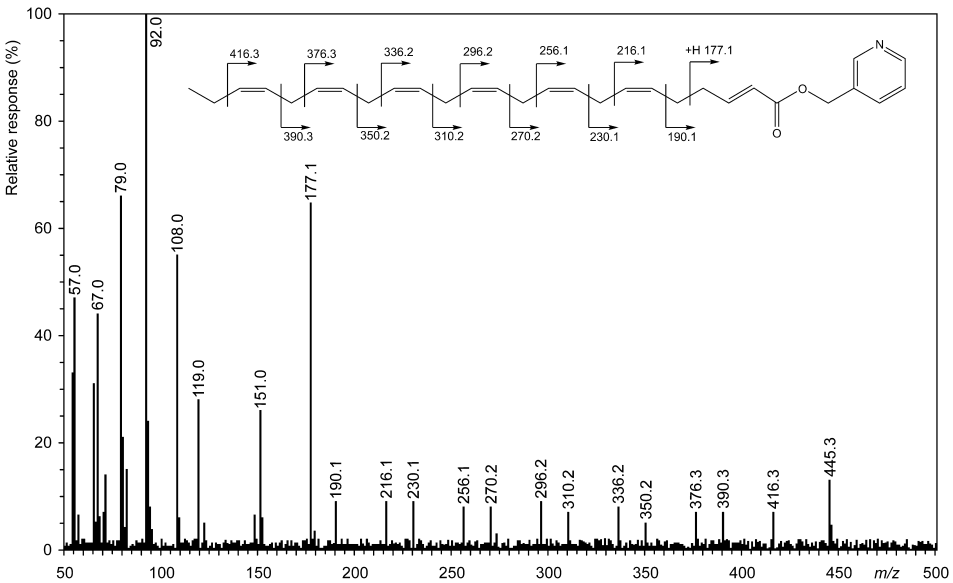

Fig. 2 The mass spectrum of 3-pyridyl carbonyl ester of 2,6,9,12,15,18,21-tetracosaheptaenoic acid

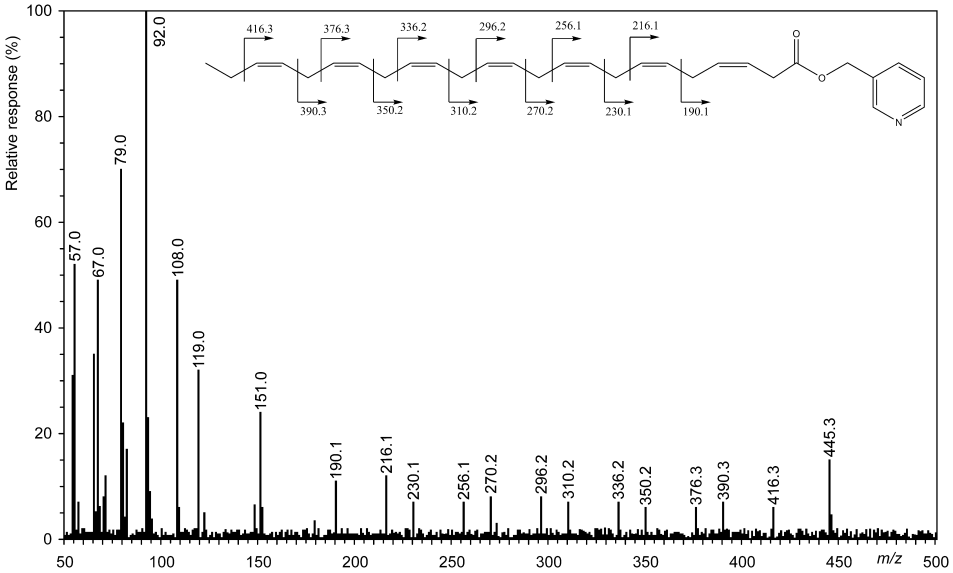

Fig. 3 The mass spectrum of 3-pyridyl carbonyl ester of 24:7n-3 acid

of ions at *m*/*z* 355.3, SIM was used to identify the acid 24:6 in neutral lipids, that is, TAG and diacylglycerol (DAG), as well as in phospholipids (PlsNAPtdEtn, NAPtdEtn, PtdEtn, PlsNAPtdSer, NAPtdSer, and PtdSer). By contrast, using SIM at 353.3, which is an ion of the $RCOO^-$ structure corresponding to 24:7, this acid was identified in both plasmenyl classes, that is, PlsNAPtdEtn and PlsNAPtdSer. The third SIM record at 426.3 Da corresponds to the structure of the *N*-arachidonoyl ethanolamide phosphate anion, which was only identified in the molecular species of ethanolamines (PlsNAPtdEtn and/or NAPtdEtn). Using NLS 373.3 Da, several molecular species of *N*-arachidonoyl-

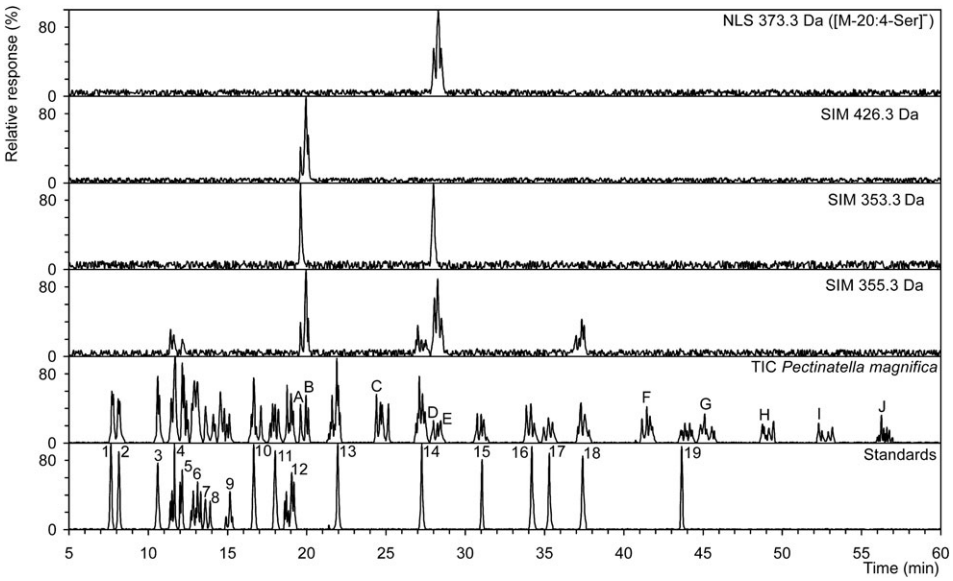

Fig. 4 High-performance liquid chromatography/electrospray ionization mass spectrometry (HPLC/ESI–MS) separation of standards (bottom) and major lipid classes of bryozoan. Selected-ion monitoring (SIM) at 355.3, 353.3, and 426.3 Da of 24:6, natural 24:7 polyunsaturated fatty acid (PUFA), *N*-acyl ethanolamide phosphate anion, and neutral-loss scanning (NLS) 373.3 (20:4-serine) from total lipids of *P. magnifica.* Identification of peaks (peak no.; RT; lipid classes): (1; 7.65; hydrocarbons), (2; 8.15; squalen), (3; 10.60; sterol esters), (4; 11.65; triacylglycerol [TAG]), (5; 12.25; diacylglycerol [DAG]), (6; 13.05; monogalactosyldiacylglycerols), (7; 13.60; sterols), (8; 13.90; free fatty acid [FA]), (9; 15.15; sulfoquinovosyldiacylglycerols), (10; 16.65; diacylglycerylhydroxymethyl trimethylalanine/diacylglyceryltrimethylhomoserine), (11; 18.00; phosphatidylglycerols), (12; 18.95; digalactosyldiacylglycerols), (A; 19.60; plasmenyl-*N*-acyl-ethanolamine phospholipids), (B; 19.95; *N*-acyl-ethanolamine phospholipids), (13; 21.95; phosphatidylcholines [PtdCho]), (C; 24.40; unknown 1), (14; 27.25; PtdEtn), (D; 27.95; plasmalogens-*N*-acylphosphatidylserines), (E; 28.25; *N*-acylphosphatidylserines), (15; 31.00; lysophosphatidylcholines), (16; 34.15; phosphatidylinositols), (17; 35.35; phosphatidic acids [PtdOH]), (18; 37.35; phosphatidylserines [PtdSer]), (F; 41.45; unknown 2), (19; 43.65; lysophosphatidic acids), (G; 45.10; unknown 3), (H; 48.75; unknown 4), (I; 52.30; unknown 5), and (J; 56.25; unknown 6)

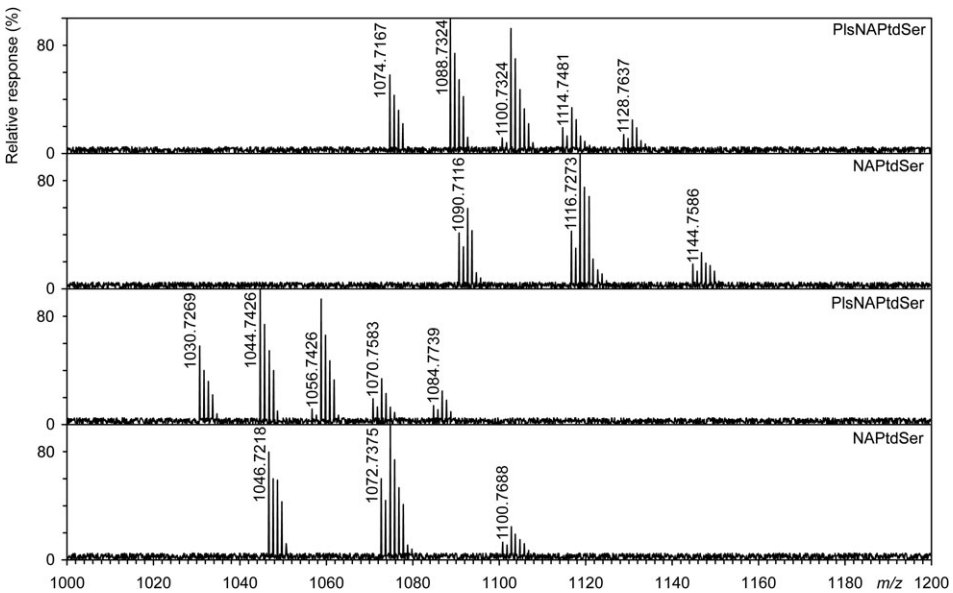

Fig. 5 Negative-ion electrospray ionization mass spectrometry (ESI–MS) analysis of lipids eluting from *P. magnifica* in the interval 19.55–19.75 min (plasmenyl-*N*-acylphosphatidylethanolamine [PlsNAPtdEtn]), 19.80–20.25 min (*N*-acylphosphatidylethanolamine [NAPtdEtn]), 27.80–28.10 min (plasmenyl-*N*-acylphosphatidylserine [PlsNAPtdSer]), and 28.15–28.70 min (*N*-acylphosphatidylserine [NAPtdSer])

PtdSer, including alkenyl-acyl and diacyl-NAPtdSer, were also identified. The neutral loss value of 373.3 Da corresponds to the loss of a neutral molecule with the structure of 20:4-dehydroalanine (20:4-serine).

Negative-ion ESI tandem MS was used to characterize the structure of each class of phospholipids and to identify the molecular species including regioisomers. The major phospholipid ions in the negative ESI–MS^2 include mainly the deprotonated molecular ion $[M - H]^-$. Fig. 5a–d shows the presence of multiple *N*-acyl-phospholipid ion species (1000–1200 Da) in the negative-ion high-resolution ESI mass spectra of bryozoan lipids eluting from the HILIC column. The *N*-acyl-phospholipid structures were proposed based on MS^2 and high-resolution MS. Fig. 5 shows the high-resolution tandem mass spectra of $[M - H]^-$ ions of four *N*-acyl phospholipids in the following intervals 19.55–19.80 (PlsNAPtdEtn), 19.90–20.20 (NAPtdEtn), 27.80–28.10 (PlsNAPtdSer), and 28.15–28.70 (NAPtdSer), and from 1000 to 1200 Da, that is, the area of $[M - H]^-$ ions. Appropriate molecular species are shown in Table 2a–d. Other isobaric molecular species listed in the tables were similarly identified. Table 2a–d further summarizes the *m/z* values, the abundance of ions, and the description of individual molecular species.

The low percentages for some molecules may be caused by the isotopic distribution of other molecules, which contributes to the fact that some molecules have a lower representation than is actually the case. We believe, however, that this phenomenon is not very pronounced. The above target mass resolution (full width at half maximum [FWHM]) 105,000 at *m/z* 800 is insufficient, for example, for the complete separation of $[M - H]^-$ ions at *m/z* 1150.8055 (NAPtdSer-18:0/24:5/20:4) and $[M - H + 2]^-$ ions at *m/z* 1150.7962 (NAPtdSer-18:0/24:6/20:4). The difference was 0.0093 Da, and the required FWHM would be at *m/z* 1150 of about 126,000. Yet some indication of separation was apparent. We determined a ratio of 17.2:2.7 by manual counting (see Table 2a–d).

Analysis of Phospholipids in the Negative Mode

NAPtdEtn

A group of major fragment ions in the negative ESI tandem MS spectrum is presented in Tables S1–S4 and Fig. 6. The ions at *m/z* 255.2331 and 329.2486 represent the FA carboxylate anions of palmitic and docosapentaenoic acid, respectively. The carboxylate anion at *m/z* 329.2486 originating from the *sn*-2 position is more abundant than the carboxylate anion at *m/z* 255.2331 originating from *sn*-1. On the basis of these data, we, therefore, assumed that NAPtdEtn was esterified in the *sn*-1 position with palmitic and in *sn*-2 with docosapentaenoic acids. The spectrum also contained four ions at 720.4973 and 794.5131 Da, corresponding to two neutral losses of acids, and another pair at 738.5079 and 812.5236 Da belonging to neutral loss acids in the form of ketenes.

Particularly for NAPtdEtn, the characteristic neutral loss of a FA from the glycerophosphoric backbone is followed by further fragmentation of the phosphoric acid ester under neutral loss of the *N*-arachidonoylethanolamine moiety. This results in two ions at 465.2417 Da (neutral loss of

Table 2 Abundances of molecular species of (a) *N*-acylphosphatidylethanolamine (NAPtdEtn), (b) plasmenyl-*N*-acylphosphatidylethanolamine (PlsNAPtdEtn), (c) *N*-acylphosphatidylserines (NAPtdSer), and (d) plasmenyl-*N*-acylphosphatidylserines (PlsNAPtdSer) from *P. magnifica* determined using mass spectrometry

$[M-H]^-$	Molecular species[a] *sn*-1/*sn*-2/*N*-acyl	Abundance	Molecular species	Abundance	Molecular species	Abundance	Molecular species	Abundance	Molecular species	Abundance	Sum of abundances[b]
(a) NAPtdEtn											
1046.7218	16:0/22:6/20:5	79.7[a]									79.7
1048.7375	16:0/22:6/20:4	16.1	16:0/22:5/20:5	42.9							59.0
1050.7531	16:0/22:5/20:4	8.6									8.6
1072.7375	18:1/22:6/20:5	60.0									60.0
1074.7531	16:0/24:6/20:5	23.9	18:0/22:6/20:5	31.8	18:1/22:6/20:4	32.2	18:1/22:5/20:5	12.1			100.0
1076.7687	16:0/24:6/20:4	9.4	18:0/22:6/20:4	17.1	16:0/24:5/20:5	14.0	18:0/22:5/20:5	6.4	18:1/22:5/20:4	6.5	53.4
1078.7844	16:0/24:5/20:4	7.6	18:0/22:5/20:4	3.4							11.0
1100.7688	18:1/24:6/20:5	13.1									13.1
1102.7844	18:0/24:6/20:5	6.9	18:1/24:6/20:4	7.0	18:1/24:5/20:5	10.6					24.5
1104.8001	18:0/24:6/20:4	3.7	18:0/24:5/20:5	5.6	18:1/24:5/20:4	5.7					15.0
1106.8157	18:0/24:5/20:4	3.0									3.0

$[M-H]^-$	Molecular species[a] *sn*-1/*sn*-2/*N*-acyl	Abundance	Molecular species	Abundance	Molecular species	Abundance	Sum of abundances
(b) PlsNAPtdEtn							
1030.7269	16:0/22:6/20:5	58.1					58.1
1032.7425	16:0/22:6/20:4	31.9					31.9
1044.7426	17:0/22:6/20:5	100.0					100.0
1046.7582	17:0/22:6/20:4	54.6					54.6
1056.7426	16:0/24:7/20:5	11.5					11.5
1058.7582	16:0/24:7/20:4	6.4	16:0/24:6/20:5	13.9	18:0/22:6/20:5	72.1	92.4
1060.7738	16:0/24:6/20:4	7.7	18:0/22:6/20:4	39.5			47.2
1070.7583	17:0/24:7/20:5	19.1					19.1
1072.7739	17:0/24:7/20:4	10.7	17:0/24:6/20:5	23.2			33.9
1074.7895	17:0/24:6/20:4	12.9					12.9
1084.7739	18:0/24:7/20:5	14.0					14.0
1086.7895	18:0/24:7/20:4	7.8	18:0/24:6/20:5	17.0			24.8
1088.8051	18:0/24:6/20:4	9.5					9.5

[M − H]⁻	Molecular species[a] *sn*-1/*sn*-2/*N*-acyl	Abundance	Molecular species	Abundance	Molecular species	Abundance	Molecular species	Abundance	Molecular species	Abundance	Sum of abundances
(c) NAPtdSer											
1090.7116	16:0/22:6/20:5	41.3									41.3
1092.7273	16:0/22:6/20:4	27.8	16:0/22:5/20:5	31.6							59.4
1094.7429	16:0/22:5/20:4	11.9									11.9
1116.7273	18:1/22:6/20:5	42.6									42.6
1118.7429	16:0/24:6/20:5	30.0	18:0/22:6/20:5	38.9	18:1/22:6/20:4	22.5	18:1/22:5/20:5	8.6			100.0
1120.7585	16:0/24:6/20:4	16.5	18:0/22:6/20:4	22.4	16:0/24:5/20:5	11.9	18:0/22:5/20:5	10.1	18:1/22:5/20:4	7.3	68.2
1122.7742	16:0/24:5/20:4	9.4	18:0/22:5/20:4	4.6							14.0
1144.7586	18:1/24:6/20:5	18.3									18.3
1146.7742	18:0/24:6/20:5	4.7	18:1/24:6/20:4	5.7	18:1/24:5/20:5	16.3					26.7
1148.7899	18:0/24:6/20:4	5.1	18:0/24:5/20:5	7.2	18:1/24:5/20:4	4.9					17.2
1150.8055	18:0/24:5/20:4	2.7									2.7

[M − H]⁻	Molecular species[a] *sn*-1/*sn*-2/*N*-acyl	Abundance	Molecular species	Abundance	Molecular species	Abundance	Sum of abundances
(d) PlsNAPtdSer							
1074.7167	16:0/22:6/20:5	46.0					58.1
1076.7323	16:0/22:6/20:4	38.2					31.9
1088.7324	17:0/22:6/20:5	89.5					100.0
1090.7480	17:0/22:6/20:4	100.0					54.6
1100.7324	16:0/24:7/20:5	14.6					11.5
1102.7480	16:0/24:7/20:4	5.8	16:0/24:6/20:5	16.7	18:0/22:6/20:5	65.4	92.4
1104.7636	16:0/24:6/20:4	9.3	18:0/22:6/20:4	42.4			47.2
1114.7481	17:0/24:7/20:5	17.9					19.1
1116.7637	17:0/24:7/20:4	15.2	17:0/24:6/20:5	26.8			33.9
1118.7793	17:0/24:6/20:4	11.3					12.9
1128.7637	18:0/24:7/20:5	17.8					14.0
1130.7793	18:0/24:7/20:4	6.7	18:0/24:6/20:5	15.6			24.8
1132.7949	18:0/24:6/20:4	10.4					9.5

[a]Arithmetic means from three cultivations ± *SD*.

[b]Calculated as a percentage of individual peak areas divided by the total area of the extracted ion profile (i.e. MS1 trace).

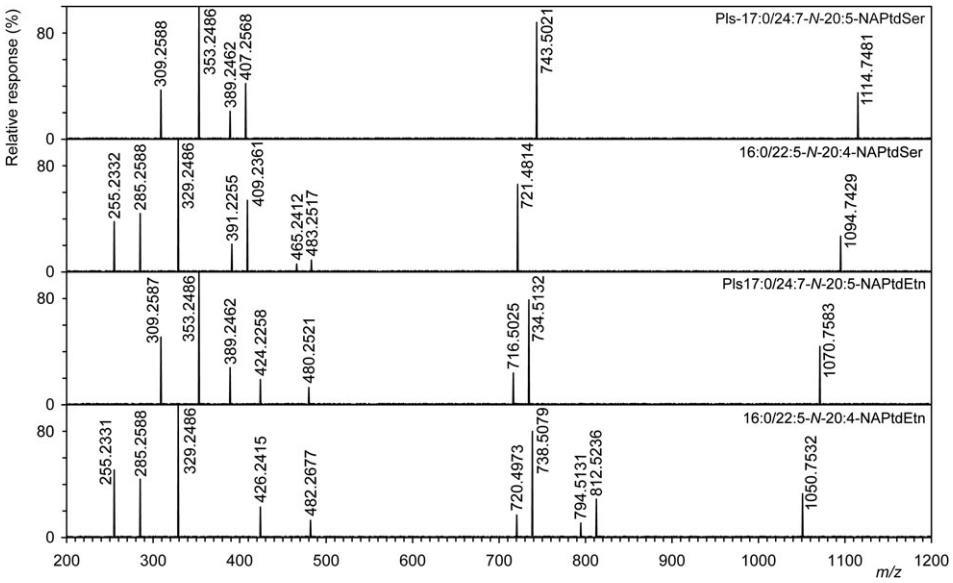

Fig. 6 Tandem negative high-resolution mass spectra of four phospholipids, that is, Pls-17:0/24:7-*N*-20:5-*N*-acylphosphatidylserine (NAPtdSer), 16:0/22:5-*N*-20:4-NAPtdSer, Pls-17:0/24:7-*N*-20:5-*N*-acylphosphatidylethanolamine (NAPtdEtn), and 16:0/22:5-*N*-20:4-NAPtdEtn

palmitic acid) from the *sn*-1 position and an ion at 391.2260 Da (neutral loss of docosapentaenoic acid from the *sn*-2 position). The ion at 391.2260 Da has a higher abundance than the ion at 465.2417 Da, thus confirming regiostereospecificity, that is, the acyl at the *sn*-1 position is palmitic and that at *sn*-2 is docosapentaenoic acid.

PlsNAPtdEtn

Negative ESI–MS of plasmenyl NAPtdEtn (PlsNAPtdEtn) shows a homologous sequence. As an example, we present the identification of $[M - H]^-$ ions by MS^2 at 1070.7583 Da. Tandem MS reveals an abundant ion at *m/z* 353.2486 belonging to the corresponding R_2COO^- and, as is common with PUFA, also an ion having a 44 Da lower mass produced by the cleavage of CO_2 from the $RCOO^-$ ion, where the acid esterifies the *sn*-2 position of the glycerol backbone. Furthermore, both neutral loss of the *N*-heptadecanoylethanolamine moiety and loss of ketene ($R_2'CH{=}C{=}O$) and FA from *sn*-2 results in the formation of ions at 734.5132 and 716.5025 Da, respectively. Thus, the structure of this plasmenyl derivative was confirmed as Pls-17:0/24:7-*N*-20:4-PtdEtn.

NAPtdSer

FA ester linked to the glycerol backbone were identified based on ions at *m/z* 329.2486 and another ion at *m/z* 285.2588 generated by CO_2 loss, a phenomenon occurring in PUFA. The ion at *m/z* 255.2332 belongs to palmitic acid. Furthermore, a majority ion was identified at *m/z* 721.4814, corresponding to phosphatidic acid (PtdOH) with two bound acids (16:0 and 22:5). An ion at *m/z* 483.2517 arises due to loss of the *sn*-1 acyl chain as ketene ($R'CH{=}C{=}O$) from the PtdOH anion while an ion at *m/z* 465.2412 is formed by neutral loss of *sn*-1 RCOOH FA from the PtdOH anion. Similarly, ions at *m/z* 409.2361 and/or 391.2255 were produced by neutral loss of 22:5 as FA and/or its ketene. For the determination of stereochemistry, it was important to compare the abundance of product ions derived from the loss of the fatty acyl substituent at *sn*-2 to the same type of ions resulting from loss at *sn*-1. Product ions at *m/z* 409.2361 and 391.2255 were more abundant than ions at *m/z* 483.2517 and 465.2412, that is, those that were generated by neutral loss from the *sn*-1 position. Thus, palmitic acid can be said to be ester-bound in the *sn*-1 position and docosapentaenoic acid in the *sn*-2 position. The PtdOH anion observed at *m/z* 721.4814 is generated during MS^2 from $[M - H]^-$ at *m/z* 1094.7429 by neutral loss of 373.2617 Da. From the odd mass of the neutral loss fragment, it is obvious that it contains an odd number of nitrogen atoms, in our case one. The exact mass of the neutral loss of 325.261 Da was determined from the difference in mass between the accurately measured $[M - H]^-$ ion and the mass of the 16:0/22:5 PtdOH anion. This elemental composition, combined with the above data of tandem MS, indicate the presence of *N*-arachidonoylphosphatidylserine in the mixture of diacyl's lipids (16:0/22:5-*N*-20:4-PtdSer).

PlsNAPtdSer

Like PlsNAPtdEtn, PlsNAPtdSer were identified in total lipids. A representative tandem MS spectrum is shown in Fig. 6, where the plasmenyl NAPtdSer shows an abundant

molecular $[M - H]^-$ ion at *m/z* 1114.7481 and a prominent ion at *m/z* 743.5021 arising due to the neutral loss of *N*-eicosapentaenoyl PtdSer (chemical formula $C_{23}H_{33}NO_3$, exact mass 371.2461 Da), which is essentially alkenyl/acyl-phosphatidic acid. Thus, the *N*-acyl moiety was identified. The ion at 353.2486 Da demonstrates the presence of an ion of structure R_2COO^-, where the corresponding FA is 24:7. This ion is accompanied by an ion at 309.2588 Da, which corresponds to the structure of $R_2COO{-}CO_2$. In addition, there are pairs of ions at 407.2568 and 389.2462 Da, which result from the loss of ketene or acid from the PtdOH anion. Unfortunately, we again did not detect the corresponding plasmenyl ion at *sn*-1 of the glycerol backbone.

Discussion

Fatty Acids

As already mentioned in "Introduction," our results in Table 1 can essentially be compared with only a very small number of published papers. In essence, three FA, 16:0, 20:5n-3, and 22:6n-3, are present in most of the bryozoans regardless of whether they live in seawater or freshwater, and account for at least one-third of the total FA content. In addition, even-numbered PUFA of 16–22 carbon atoms are present, namely C16 and C18 with two to four double bonds, C20–C22 with up to six double bonds, and also VLCPUFA, that is, 24:6n-3 and 24:4n-3. The presence of two demospongic acids (5,9,19–26:3 and 5,9,19–28:3) is explained by the contamination of the bryozoans by a sponge (Demidkova, 2010). Nonmethylene interrupted FA, that is, 5,11–20:2, 7,13–20:2, and 7,13–22:2, and many others have also been identified (Demidkova, 2010). They have been confirmed only in marine bryozoans and have not been proven either in our work or by Makhutova et al. (2016). It is possible to speculate that their presence is a taxonomic marker of marine bryozoans. However, there are insufficient experimental data for this claim. Can they come from food? Freshwater and marine plankton fairly differ in their composition.

Other C24 PUFA identified in *P. magnifica* included two pairs of positional isomers 24:4 (n-3 and n-6) and 24:5 (n-3 and n-6), 24:6 and very rarely occurring 24:7n-3 (all-*cis*-3,6,9,12,15,18,21–24:7; (3*Z*,6*Z*,9*Z*,12*Z*,15*Z*,18*Z*,21*Z*)-tetracosa-3,6,9,12,15,18,21-heptaenoic acid). Nisinic acid, despite its less common structure, is widespread. In particular, it is an important biosynthetic intermediate in the biosynthesis of 22:6n-3, by the Sprecher pathway (Sprecher, Luthria, Mohammed, & Baykousheva, 1995) in vertebrates, from fish to mammals. The presence of this acid in invertebrates has also been described several times, for example, in the bryozoan *Flustra* sp. (Vysotskii & Svetashev, 1996), in the soft coral *Gersemia rubiformis* (Imbs & Dang, 2017), and many others, see the paper of Suo et al. (2015).

A completely different situation is with 24:7n-3, where we only found a very old mention of the presence of this acid in bonito oil (Matsuda, 1942) describing the presence of C24 acid with seven double bonds. Unfortunately, our search from September 19, 2017, in the SciFinder (Chemical Abstracts) database was negative. Therefore, we believe that this acid has not yet been described.

Phospholipids

The analysis of phospholipids or their molecular species has already been dealt with by many articles, including several reviews. As mentioned above, the biosynthetic precursors of endocannabinoids, especially anandamide, are *N*-arachidonoyl-PtdEtn compounds or other *N*-acyl-PtdEtn (e.g. *N*-palmitoyl- and *N*-stearoyl-ethanolamide). Their analysis in mammalian tissues, predominantly in the brain, has been described many times (Astarita et al., 2008; Guan, 2009; Guan et al., 2007; Hansen et al., 1999). Essentially, this always involves the separation or enrichment of *N*-acyl phospholipids, followed by identification and quantification by MS. The NAPtdEtn content is usually very low; for instance, Wellner, Diep, Janfelt, and Hansen (2013) estimated their content at ~0.01% of total phospholipids. The content we found in the bryozoan is two orders higher. The use of the negative HR-ESI–MS^2 led to the identification of dozens of molecular species; besides diacyl we also identified plasmenyl-acyl-NAPtdEtn and -NAPtdSer (see Table 2a–d). The ions resulting from the fragmentation in the MS^2 (see Tables S1–S4) are the same as those already published (Astarita et al., 2008; Guan, 2009; Guan et al., 2007; Hansen et al., 1999).

Based on the measured values, it was found that the alkenyl group in the alkenyl/acyl-*N*-acyl-PtdEtn and/or PtdSer was not subjected to fragmentation in MS^2, the major difference between diacyl-NAPtdEtn and alkenyl-acyl-NAPtdEtn being consistent with the previously published data obtained from ESI–MS experiments performed with diacyl-PtdEtn or alkenyl-acyl-PtdEtn, respectively (Hsu & Turk, 2009). This suggests that alkenyl/acyl-NAPtdEtn can be identified by the absence of a carboxylate anion originating from the *sn*-1 position in ESI MS^2. Generally, negative ESI MS^2 gives rise to a characteristic fragmentation similar to that of ethanolamine glycerophospholipids showing carboxylate anions after deacylation of the glycerophosphoethanolamine backbone, and the corresponding fragments containing the deprotonated phosphate group. In all analyses, however, it has to be taken into account that the higher molecular weight of the NAPtdEtn precursor ions is due to the *N*-acylation of the primary amino group. After

fragmentation, this acyl group as such is not identified in MS^2 (no amide bond cleavage occurs), but the neutral loss gives rise to *N*-acylethanolamine moieties.

The quantitative representation of individual molecular species naturally differs. For example, the bacterium *Bdellovibrio* contains NAPtdEtn in which at least one of the three FA at the *sn*-1, *sn*-2, or *N*-acyl positions is C17 or C19 cyclopropane FA (Muller, Beck, Strauch, & Linscheid, 2011). Triebl, Weissengruber, Trotzmuller, Lankmayr, and Kofeler (2016) described dozens of molecular species in the rat brain, where *N*-acyl is formed by either saturated FA (16:0 or 18:0) or PUFA (20:4 or 22:6). In another work on rat brain, some *N*-arachidonoyl-PtdEtn were quantitated. For instance, the molecular species 18:0/22:6-*N*-20:4 was found at 51 pmol/1 g wet tissue, which is about 55 ng/1 g. The quantity of the same molecular species that we found is 210 times higher. Very unusual molecular species, that is, those containing VLCPUFA, have been identified in macrophage cells; here diacyl, plasmenyl-acyl, and plasmanyl-acyl are formed by C24 and C26 PUFA, that is, 24:3 to 24:6 and/or higher homologs such as 26:3 to 26:6 (Ivanova, Milne, & Brown, 2010). It is generally accepted (Rezanka & Sigler, 2009) that odd-numbered FA are present in considerable quantities predominantly in lower organisms. This fact was fully confirmed in *P. magnifica*, since plasmenyl-lipids contained the C17 hydrocarbon chain as the plasmenyl derivative in a substantial amount (see Table 1) (analyzed as DMA). This finding is in line with the previously published data (Berdyshev et al., 1992), where heptadecanal was found to be one of the major aldehydes in bryozoa and its content was more than 35% of total aldehydes. At present, analysis of molecular species of lipids from lower animals is only in its beginning and the number of publications using lipidomic analysis is negligible. Thus Imbs and Dang (2017) identified 68 molecular species of PtdEtn, PtdSer, phosphatidylcholines (PtdCho), and phosphatidyl inositols (PtdIns) in the cold-water soft coral *G. rubiformis* from the Sea of Okhotsk. The alkenyl-acyl and diacyl type molecular species contained 24:5 and 24:6 in the *sn*-2 position. Analysis of the phospholipid molecular species composition of the soft coral *Xenia* sp. from the South China Sea revealed molecular species of PtdIns containing 24:5 or 24:6 FA (e.g. 16:0/24:5, 18:0/24:6, 18:0/24:5) (Imbs, Dang, Rybin, & Svetashev, 2015). Garrett, Schmeitzel, Klein, Hwang, and Schwarz (2013) identified in the sea anemone *Aiptasia pallida* the diacyl and plasmenyl derivatives of PtdIns, PtdSer, and 1-O-alkenyl-2-acyl-*sn*-glycero-3-phosphoethanolamine or ethanolamine plasmalogen that contained PUFA in the *sn*-2 position. The phospholipid composition of the freshwater bryozoan we analyzed can thus be seen to be similar to that of other lower invertebrates, including those from the marine environment.

The cannabinoid research in invertebrate animals is interesting and potentially important in that it can reveal the role of these compounds in diverse functions, so far poorly understood and studied, of relatively primitive organisms that may eventually help to spur progress in understanding the function of the nervous system in higher organisms including mammals. For instance, *N*-acylphosphatidylethanolamines, including anandamide, palmitoyl-, and stearoylethanolamines, identified in lipid extracts from the sea urchin *Paracentrotus lividus* may act as oocyte-derived cannabimimetic regulators of sea urchin fertility (Bisogno et al., 1997) while several long-chain *N*-acylethanolamines, including the proposed endogenous ligands of cannabinoid receptors, anandamide, and *N*-palmitoylethanolamine, as well as some of their putative biosynthetic precursors, *N*-acylphosphatidylethanolamines, found in bivalve molluscs (Sepe, De Petrocellis, Montanaro, Cimino, & Di Marzo, 1998) have been assumed to play an immunomodulatory role in the bivalve. The endocannabinoid signaling system in *Hydra* sp. (Cnidaria) is assumed to play a physiological role in controlling the feeding response (De Petrocellis, Melck, Bisogno, Milone, & Di Marzo, 1999) and the possible physiological function of the endocannabinoid system in the sea squirt *Ciona intestinalis* is the control of a typical reflex response (Matias, McPartland, & Di Marzo, 2005). Knowledge of the endocannabinoid signaling including its evolution and comparative neurobiology is thus intrinsically interesting and has great potential for both pure and applied research.

P. magnifica, obviously an invasive species, can grow up to reach amounts of several metric cents of wet weight in one pond or sand pit. An amount of 25 g dry matter, that is, 2.5%, was obtained by freeze-drying, from 1 kg of wet mass of the bryozoan. In this dry matter, the total lipid content was about 15%. The individual lipid classes participating in total lipids are shown in Fig. 4, the amount of the endocannabinoid precursor NAPtdEtn being 2.1%. For example, the concentration of the molecular species 18:0/22:6-*N*-20:4 in rat brain can be calculated at 51 pmol/g wet tissue (Astarita et al., 2008), which is about 55 μg/kg. In *P. magnifica*, the same molecular species was present in an amount of more than two orders of magnitude higher, that is, 11.6 mg/1 kg wet weight.

Acknowledgements This research was supported by GACR project 17-00027S and by Institutional Research Concepts RVO61388971.

References

Astarita, G., Ahmed, F., & Piomelli, D. (2008) Identification of biosynthetic precursors for the endocannabinoid anandamide in the rat brain. *Journal of Lipid Research*, **49**:48–57.

Balounová, Z., Rajchard, J., Švehla, J., & Šmahel, L. (2011) The onset of invasion of bryozoan *Pectinatella magnifica* in South Bohemia (Czech Republic). *Biologia*, **66**:1091–1096.

Berdyshev, E. V., Getmanova, O. E., Svetashev, V. I., & Kubanin, A. A. (1992) The heptadecanoic fatty aldehyde—One of the main aldehydes of the Far-Eastern Bryozoa. *Comparative Biochemistry and Physiology*, **102B**:639–641.

Bisogno, T., Ventriglia, M., Milone, A., Mosca, M., Cimino, G., & Di Marzo, V. (1997) Occurrence and metabolism of anandamide and related acyl-ethanolamides in ovaries of the sea urchin *Paracentrotus lividus*. *Biochimica et Biophysica Acta*, **1345**:338–348.

Bligh, E. G., & Dyer, W. J. (1959) A rapid method of total lipid extraction and purification. *Canadian Journal of Biochemistry and Physiology*, **37**:911–917.

Braverman, N. E., & Moser, A. B. (2012) Functions of plasmalogen lipids in health and disease. *Biochimica et Biophysica Acta*, **1822**: 1442–1452.

Christie, W. W. (2003) *Lipid analysis*. Bridgwater: The Oily Press.

Christie, W. W. (2017) *The lipid home.* Retrieved from http://www.lipidhome.co.uk

De Petrocellis, L., Melck, D., Bisogno, T., Milone, A., & Di Marzo, V. (1999) Finding of the endocannabinoid signalling system in *Hydra*, a very primitive organism: Possible role in the feeding response. *Neuroscience*, **92**:377–387.

Demidkova, D. A. (2010) The composition of fatty acids and aldehydes of the marine bryozoans *Berenicea meandrina* and *Dendrobeania flustroides* (Bryozoa: Gymnolaemata). *Russian Journal of Marine Biology*, **36**:300–304.

Fellenberg, A. J., Johnson, D. W., Poulos, A., & Sharp, P. (1987) Simple mass-spectrometric differentiation of the normal-3, normal-6 and normal-9 series of methylene interrupted polyenoic acids. *Biomedical & Environmental Mass Spectrometry*, **14**: 127–129.

Garrett, T. A., Schmeitzel, J. L., Klein, J. A., Hwang, J. J., & Schwarz, J. A. (2013) Comparative lipid profiling of the cnidarian *Aiptasia pallida* and its dinoflagellate symbiont. *PLoS One*, **8**: e57975.

Goldfine, H. (2010) The appearance, disappearance and reappearance of plasmalogens in evolution. *Progress in Lipid Research*, **49**: 493–498.

Guan, Z. (2009) Discovering novel brain lipids by liquid chromatography/tandem mass spectrometry. *Journal of Chromatography, B: Analytical Technologies in the Biomedical and Life Sciences*, **877**: 2814–2821.

Guan, Z., Li, S., Smith, D. C., Shaw, W. A., & Raetz, C. R. H. (2007) Identification of N-acylphosphatidylserine molecules in eukaryotic cells. *Biochemistry*, **46**:14500–14513.

Hansen, H. H., Hansen, S. H., Bjørnsdottir, I., & Hansen, H. H. (1999) Electrospray ionization mass spectrometric method for the determination of cannabinoid precursors: N-acylethanolamine phospholipids (NAPtdEtns). *Journal of Mass Spectrometry*, **34**: 761–767.

Hsu, F. F., & Turk, J. (2009) Electrospray ionization with low-energy collisionally activated dissociation tandem mass spectrometry of glycerophospholipids: Mechanisms of fragmentation and structural characterization. *Journal of Chromatography B*, **877**:2673–2695.

Imbs, A. B., & Dang, L. T. P. (2017) The molecular species of phospholipids of the cold-water soft coral *Gersemia rubiformis* (Ehrenberg, 1834) (Alcyonacea, Nephtheidae). *Russian Journal of Marine Biology*, **43**:239–244.

Imbs, A. B., Dang, L. T. P., Rybin, V. G., & Svetashev, V. I. (2015) Fatty acid, lipid class, and phospholipid molecular species composition of the soft coral *Xenia* sp. (Nha Trang Bay, the South China Sea, Vietnam). *Lipids*, **50**:575–589.

Ivanova, P. T., Milne, S. B., & Brown, H. A. (2010) Identification of atypical ether-linked glycerophospholipid species in macrophages by mass spectrometry. *Journal of Lipid Research*, **51**:1581–1590.

Kates, M., & Volcani, B. E. (1996) Biosynthetic pathways for phosphatidylsulfocholine, the sulfonium analogue of phosphatidylcholine, in diatoms. In M. D. Keller, R. P. Kiene, G. O. Kirst, & P. T. Visscher (Eds.), *Biological and environmental chemistry of DMSP and related sulfonium compounds* (pp. 109–119). New York, NY: Plenum Press.

Lehtonen, M., Reisner, K., Auriola, S., Wong, G., & Callaway, J. C. (2008) Mass-spectrometric identification of anandamide and 2-arachidonoylglycerol in nematodes. *Chemistry & Biodiversity*, **5**: 2431–2441.

Lucanic, M., Held, J. M., Vantipalli, M. C., Klang, I. M., Graham, J. B., Gibson, B. W., … Gill, M. S. (2011) N-acylethanolamine signalling mediates the effect of diet on lifespan in *Caenorhabditis elegans*. *Nature*, **473**:226–229.

Makhutova, O. N., Shulepina, S. P., Sharapova, T. A., Dubovskaya, O. P., Sushchik, N. N., Baturina, M. A., … Gladyshev, M. I. (2016) Content of polyunsaturated fatty acids essential for fish nutrition in zoobenthos species. *Freshwater Science*, **35**:1222–1234.

Massard, J. A., & Geimer, G. (2007) Global diversity of bryozoans (Bryozoa or Ectoprocta) in freshwater. *Hydrobiologia*, **595**:93–99.

Matias, I., McPartland, J. M., & Di Marzo, V. (2005) Occurrence and possible biological role of the endocannabinoid system in the sea squirt *Ciona intestinalis*. *Journal of Neurochemistry*, **93**: 1141–1156.

Matsuda, S. (1942) Isolation of bonitonic acid $C_{24}H_{34}O_2$ and its constitution. *Journal of the Society of Chemical Industry*, **45**:159–161.

McPartland, J. M., Matias, I., Di Marzo, V., & Glass, M. (2006) Evolutionary origins of the endocannabinoid system. *Gene*, **370**:64–74.

Muller, F. D., Beck, S., Strauch, E., & Linscheid, M. W. (2011) Bacterial predators possess unique membrane lipid structures. *Lipids*, **46**:1129–1140.

Nagan, N., & Zoeller, R. A. (2001) Plasmalogens: Biosynthesis and functions. *Progress in Lipid Research*, **40**:199–229.

Rezanka, T. (1990) Identification of very long polyenoic acids as picolinyl esters by Ag^+ ion-exchange high-performance liquid-chromatography, reversed-phase high-performance liquid-chromatography and gas-chromatography mass-spectrometry. *Journal of Chromatography*, **513**:344–348.

Rezanka, T. (1993) Polyunsaturated and unusual fatty-acids from slime-molds. *Phytochemistry*, **33**:1441–1444.

Rezanka, T., & Sigler, K. (2009) Odd-numbered very-long-chain fatty acids from the microbial, animal and plant kingdoms. *Progress in Lipid Research*, **48**:206–238.

Salzet, M., & Stefano, G. B. (2002) The endocannabinoid system in invertebrates. *Prostaglandins, Leukotrienes & Essential Fatty Acids*, **66**:353–361.

Sepe, N., De Petrocellis, L., Montanaro, F., Cimino, G., & Di Marzo, V. (1998) Bioactive long chain N-acylethanolamines in five species of edible bivalve molluscs. Possible implications for mollusc physiology and seafood industry. *Biochimica et Biophysica Acta*, **1389**:101–111.

Sprecher, H., Luthria, D. L., Mohammed, B. S., & Baykousheva, S. P. (1995) Reevaluation of the pathways for the biosynthesis of polyunsaturated fatty acids. *Journal of Lipid Research*, **36**:2471–2477.

Suo, R., Li, H., Yoshinaga, K., Nagai, T., Mizobe, H., Kojima, K., … Gotoh, N. (2015) Generation of tetracosahexaenoic acid in benthic marine organisms. *Journal of Oleo Science*, **64**:721–727.

Triebl, A., Weissengruber, S., Trotzmuller, M., Lankmayr, E., & Kofeler, H. (2016) Quantitative analysis of N-acylphosphatidylethanolamine molecular species in rat brain

using solid-phase extraction combined with reversed-phase chromatography and tandem mass spectrometry. *Journal of Separation Science*, **39**:2474–2480.

Vysotskii, M. V., & Svetashev, V. I. (1996) Fatty acids of bryozoan *Flustra* sp. (in Russ.) *Russian Journal of Marine Biology*, **22**:55–57.

Vyssotski, M., MacKenzie, A., & Scott, D. (2009) TLC and 31P-NMR analysis of low polarity phospholipids. *Lipids*, **44**: 381–389.

Wellner, N., Diep, T. A., Janfelt, C., & Hansen, H. S. (2013) N-acylation of phosphatidylethanolamine and its biological functions in mammals. *Biochimica et Biophysica Acta*, **1831**:652–662.